

# On the Identification of Cerebral Metabolites in Localized $^1\text{H}$ NMR Spectra of Human Brain *In Vivo*

Thomas Michaelis, Klaus-Dietmar Merboldt, Wolfgang Hänicke, Michael L. Gyngell, Harald Bruhn and Jens Frahm\*

Max-Planck-Institut für biophysikalische Chemie Postfach 2841, D-3400 Göttingen, Germany

Localized  $^1\text{H}$  NMR spectra of human brain *in vivo* are affected by signal overlap, strong spin-spin coupling, and complex  $J$  modulation, and therefore differ considerably from those obtained at higher magnetic fields. This paper deals with the assignment of  $^1\text{H}$  NMR resonances of cerebral metabolites under the experimental conditions used for human investigations. Conventional 7.0-T FID spectra and 2.0 T localized, short echo time STEAM spectra ( $TE = 20$  ms) of aqueous metabolite solutions are compared to *in vivo* brain spectra of human volunteers and patients. In addition to singlet resonances from *N*-acetyl aspartate (NAA), creatines, and cholines, short echo time STEAM spectra exhibit multiplets due to the NAA aspartyl group, glutamate, taurine, and *myo*-inositol. Enhanced levels of cerebral glutamine are detected in patients with liver cirrhosis. For the first time elevated levels of brain glucose are observed in patients with diabetes mellitus.

## INTRODUCTION

Recent progress in localized  $^1\text{H}$  NMR spectroscopy has led to considerable improvement with respect to its technical feasibility, achievable spectral quality, and clinical applicability. In particular, stimulated echo (STEAM) localization sequences with short echo times reveal a large number of components in spectra of human brain *in vivo*.<sup>1-3</sup> The respective resonances are linked to cerebral metabolites that are of major relevance for the biochemistry of the functioning brain. Thus, NMR spectroscopy not only offers noninvasive strategies for a clinical diagnosis based on metabolic information, but opens the way to completely new areas of research such as *in vivo* neurochemistry in man.

In order to fully develop the recent methodological achievements into valuable tools for studies of both normal and pathological metabolism, the *spectroscopic* characterization of a localized region of tissue must be transformed into a *metabolic* characterization in terms of absolute concentrations. The first step in this direction is an unambiguous identification of metabolite resonances in spectra that are acquired under optimized experimental conditions. These conditions not only require a reliable localization technique, they further necessitate the use of short echo times to detect resonances with small  $T_2$  relaxation times and to reduce  $J$  modulation effects on strongly spin-coupled resonances. It is the purpose of this paper to identify  $^1\text{H}$  NMR visible metabolites that are observable in human brain *in vivo* using state-of-the-art NMR technology.

## METHODS

High-field  $^1\text{H}$  NMR spectra (300 MHz) of aqueous solutions (deuterium oxide) of metabolites and per-

chloric acid extracts of rat brain tissue were obtained at 7.0 T (Bruker MSL 300, Karlsruhe, Germany). The model solutions were measured at room temperature with metabolite concentrations of  $\leq 100$  mM. In all cases the pH was adjusted to 7.1-7.3 using a phosphate buffer. Spectra were acquired within 24 h of preparation. The high-field results were compared to 2.0 T (Siemens Magnetom, Erlangen, Germany) localized, water-suppressed  $^1\text{H}$  NMR spectra (84.5 MHz) of both aqueous solutions of metabolites and human subjects. The spectra were acquired using a STEAM localization sequence in conjunction with three CHESS cycles for water suppression

$$[90^\circ(\text{CHESS}) - ]_3 - 90^\circ(\text{slice 1}) - TE/2 - 90^\circ(\text{slice 2}) \\ - TM - 90^\circ(\text{slice 3}) - TE/2 - \text{STE}.$$

Technical details have been described previously.<sup>1</sup> The echo time was set to  $TE = 20$  ms and the middle interval to  $TM = 30$  ms. The second half of the stimulated echo signal STE was acquired (1024 ms) with a receiver bandwidth of  $\pm 1000$  Hz (2k complex data samples, dwell time 0.5 ms). Human brain studies were performed using the same STEAM sequence as for phantoms. Spectra were acquired within measuring times of 6.5 min accumulating either 64 scans ( $TR = 6000$  ms), 128 scans ( $TR = 3000$  ms), or 256 scans ( $TR = 1500$  ms) for signal averaging. Volumes-of-interest (VOI) of between 8 and 18 mL were localized in gray and white matter regions of the brain. Spectral processing involved zero filling to 4k data points, Gaussian multiplication of the time-domain data (1.2 Hz line-broadening), Fourier transformation, and zero and first order phase correction. In general, the spectral resolution corresponded to  $\pm 0.01$  ppm.

Localized  $^1\text{H}$  NMR spectroscopy was performed subsequent to a fast scan NMR imaging protocol<sup>4</sup> combining  $T_1$ -weighted FLASH images (eight slices,  $TE = 6$  ms,  $TR = 100$  ms, flip angle  $70^\circ$ , one excitation,

\* Author to whom correspondence should be addressed.

total measuring time 26 s) and  $T_2$ -weighted CE-FAST images (single slice,  $TE = -6$  ms,  $TR = 13.8$  ms, flip angle  $40^\circ$ , four excitations, measuring time 14 s) to determine the exact position of the VOI in all three orientations. A combined imaging and spectroscopy study was completed with a total investigational time of 45–75 min yielding spectra at two to four different locations and with at least two different repetition times. Informed consent was obtained prior to the investigations.

## RESULTS AND DISCUSSION

### $^1\text{H}$ NMR spectroscopy of cerebral metabolites

Over the past 20 years extensive  $^1\text{H}$  NMR studies have been carried out to determine the visibility of mobile cytosolic compounds in excised tissues. In particular, high-resolution NMR studies at field strengths ranging from 7 to 14 T have revealed a large number of cerebral metabolites in extracts of freeze-clamped biopsy or autopsy specimens of mammalian brain. Figure 1(a) shows a conventional free induction decay (FID) spectrum of a perchloric acid extract of rat brain tissue at 7.0 T. Detailed assignments of the resonances have been reported in the literature.<sup>5–7</sup> However, while these data may be used for the identification of *singlet resonances*, the chemical shift assignments for most multiplet structures of *spin-coupled resonances* are not transferable to lower fields. This is not due to the increased resonance linewidths in spectra of living tissue and potential complications due to signal overlap, but is caused by the influence of *strong coupling* at the relatively low field strengths of 1.0 to 4.0 T currently in use for human NMR spectroscopy.

The assignment problem is illustrated by a comparison of the high-field NMR spectrum shown in Fig. 1(a) with the 2.0 T brain spectra shown in Figs. 1(b–d). The *in vivo* spectra were obtained from an 18 mL ( $2 \times 3 \times 3 \text{ cm}^3$ ) VOI localized in the occipital gray matter of a 26-year-old volunteer. Straightforward assignments are only possible for the singlet methyl resonances of *N*-acetyl aspartate (NAA) at 2.01 ppm (taken as a reference), creatine (Cr) and phosphocreatine (PCr) at 3.03 ppm, and choline-containing compounds (Cho) at 3.22 ppm. Since these metabolite resonances exhibit relatively long  $T_2$  relaxation times,<sup>8</sup> they may be specified in spectra at long echo times as shown in Fig. 1(b) where  $TE = 270$  ms. Their chemical shifts are independent of field strength and therefore agree with both high-field studies of extracts and preceding *in vivo* studies at 1.0 T,<sup>9</sup> 1.5 T,<sup>10</sup> and 2.0 T.<sup>11</sup> On the other hand, the multi-component nature of the trimethyl ammonium resonance at 3.22 ppm is only discernible at high field strengths. Potential contributions from (glycero-) phosphorylcholine detected as prominent constituents of the phosphomonoester (and diester) resonances in proton-decoupled  $^{31}\text{P}$ -NMR studies of human brain<sup>12,13</sup> remain to be clarified. For a quantitative comparison of Figs 1(a) and (b–d), it should be noted that the NAA/creatine and choline/creatine ratios are lower in rat brain than in human brain.<sup>14</sup> A more detailed investigation of species-dependent meta-

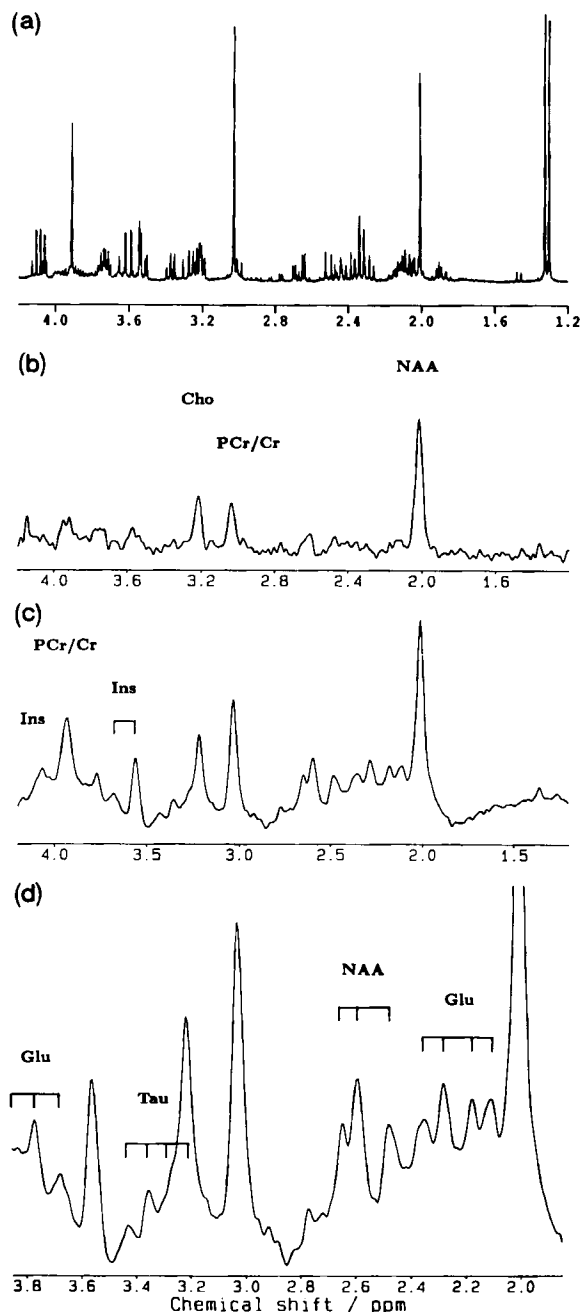


**Figure 1.**  $^1\text{H}$  NMR spectra of brain tissue under different experimental conditions: (a) 7.0 T  $^1\text{H}$  NMR spectrum of a perchloric acid (PCA) extract of rat brain, (b–d) 2.0 T  $^1\text{H}$  NMR spectra of human gray matter *in vivo* localized in a mid-sagittal position of the parietal lobe of a 26-year-old volunteer (18 mL VOI, 256 scans,  $TM = 30$  ms). Spectrum (b) represents an acquisition at an echo time of  $TE = 270$  ms ( $TR = 1600$  ms). The signal intensities are multiplied by a factor of two as compared to spectrum (c) acquired at an echo time of  $TE = 20$  ms ( $TR = 1500$  ms). Spectrum (d) is a magnified version of (c) displaying a 2.0 ppm section with the intensities being multiplied by a factor of 8/3 as compared to (c). Resonances of cerebral metabolites are due to *N*-acetyl aspartate (NAA), creatine (Cr), and phosphocreatine (PCr), choline-containing compounds (Cho), *myo*-inositol (Ins), glutamate (Glu), and taurine (Tau).

bolite concentrations in mammalian brains *in vivo* is in progress.

The quality of the  $TE = 270$  ms spectrum ( $TR = 1600$  ms, 256 scans) shown in Fig. 1(b) corresponds to previous  $^1\text{H}$  NMR studies of human brain at similar echo times where signal losses due to  $T_2$  relaxation become a dominant factor. In fact, the signal

amplitudes have been multiplied by a factor of two as compared to the spectrum shown in Fig. 1(c) acquired at a short echo time of  $TE = 20$  ms ( $TR = 1500$  ms, 256 scans). In addition to an overall improvement in signal-to-noise, the latter spectrum exhibits a considerably increased number of resonances. Most obvious are the appearance of the methylene singlet resonance of PCr/Cr at 3.94 ppm and of a strong signal from multiple collapsed resonances of *myo*-inositol (Ins) at 3.56 ppm. Resonance signals from mobile lipids and/or cytosolic proteins were generally found to be weak.<sup>1</sup> This also applies to the aromatic part of the <sup>1</sup>H NMR spectrum comprising the NAA amide proton (7.95 ppm) and the strongly coupled multiplets of adenine from adenosine triphosphate (8.0–8.5 ppm).

The spectrum shown in Fig. 1(d) represents a magnification of that in Fig. 1(c) (amplitude factor of 8/3) covering a central 2 ppm frequency range. The excellent signal-to-noise ratio and spectral resolution allows the unambiguous assignment of further strongly spin-coupled resonances of taurine, glutamate, and the aspartyl group of NAA despite the fact that the spectral patterns are completely different from those depicted at higher fields (compare Fig. 1(a)). Details of the assignments are given in subsequent sections.

The spurious signals of some of the spin-coupled metabolite resonances in spectra at longer echo times (e.g. compare Fig. 1(b)) are barely assignable and theoretically hard to predict. Since their lineshapes are determined by a complex modulation of the distorted multiplet patterns observed at short echo times, and since this pattern never fully refocuses at any particular echo time, all attempts to quantify metabolite concentrations from such signals must fail. The weakly coupled doublet resonances of the methyl groups of lactate at 1.33 ppm and alanine at 1.48 ppm represent exceptional cases in which classical  $J$  modulation yields complete refocusing of the original pattern at echo times that are multiples of  $2/J$  for stimulated echoes and  $1/J$  for spin echoes. It is therefore possible to detect these metabolites even in heavily  $T_2$ -weighted <sup>1</sup>H NMR spectra of cerebral tumors<sup>15–17</sup> and after stroke.<sup>18,19</sup> The strong lactate doublet in the *in vitro* spectrum in Fig. 1(a) is an artifact from sample preparation due to the rapid onset of anaerobic glycolysis in ischemic tissue. The low *in vivo* level of cerebral lactate in normal human subjects (compare Fig. 1(c)) as well as its variability and response to photic stimulation in the visual cortex<sup>20,21</sup> is the subject of further investigations.

### Inositol and taurine

Strong coupling occurs when the chemical shift difference  $\Delta\delta$  between two spin-coupled partners approaches the same order of magnitude as the respective spin-spin coupling constant  $J$ , i.e.,  $0.1 \leq J/\Delta\delta \leq 1$ . Since chemical shift differences in <sup>1</sup>H NMR spectra of amino acids often are within 0.1–1.0 ppm, i.e., 8–85 Hz at 2.0 T, as compared to field-independent homonuclear coupling constants of  $7 \pm 2$  Hz, strongly coupled multiplet resonances are the rule rather than the exception for most spin-coupled <sup>1</sup>H NMR resonances. The resulting multiplets exhibit major distortions relative to high-field spectra including variations in the number of resonance lines as well as in the

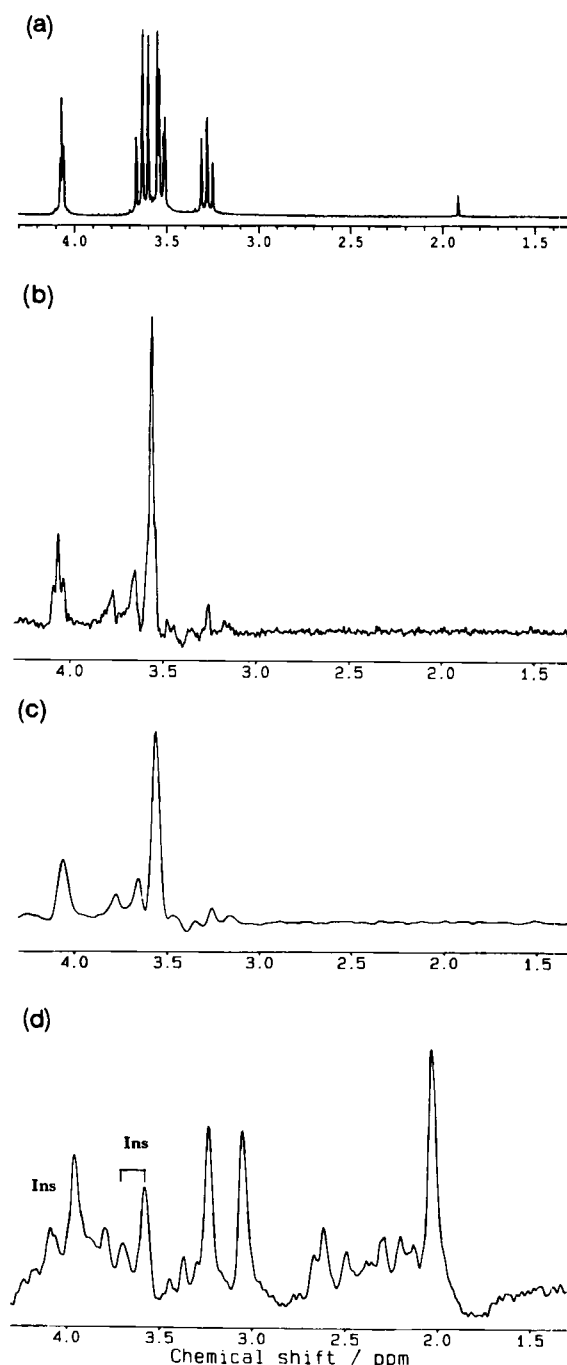


**Figure 2.** <sup>1</sup>H NMR spectra of an aqueous solution of *myo*-inositol at (a) 7.0 T and (b, c) 2.0 T in comparison to (d) a 2.0 T <sup>1</sup>H NMR spectrum of human brain *in vivo*: (a) fully relaxed FID spectrum of *myo*-inositol (pH 7.1, 50 mM, 7.0 T, \* acetate reference), (b) fully relaxed, localized STEAM spectrum of *myo*-inositol (8 mL VOI,  $TE = 20$  ms, pH 7.1, 100 mm in a 250 mL beaker, 2.0 T), and (c) linebroadened version of spectrum (b) to mimic the linewidths obtained in spectra of human brain *in vivo*. (d) <sup>1</sup>H NMR spectrum of human brain *in vivo* localized in the thalamus of a 4-year-old patient without pathological findings (8 mL VOI,  $TE = 20$  ms,  $TR = 1500$  ms, 256 scans, 2.0 T).

intensities and chemical shift values. A further consequence is the distortion of the linear relationship between peak area and number of spins which needs to be accounted for when evaluating metabolite concentrations.

Impressive examples for the qualitative spectral alterations that have to be dealt with in low-field *in vivo* NMR spectra are demonstrated in Figs 2 and 3 for *myo*-

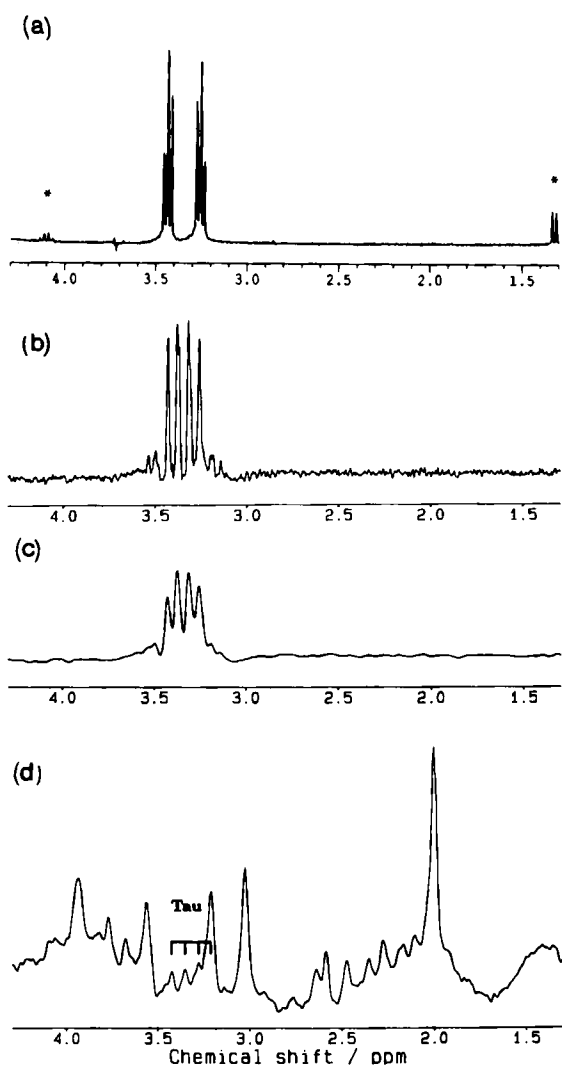


**Figure 3.**  $^1\text{H}$  NMR spectra of an aqueous solution of taurine at (a) 7.0 T and (b, c) 2.0 T in comparison to (d) a 2.0 T  $^1\text{H}$  NMR spectrum of human brain *in vivo*: (a) fully relaxed FID spectrum of taurine (pH 7.2, 50 mm, 7.0 T, \* lactate reference), (b) fully relaxed, localized STEAM spectrum of taurine (8 mL VOI,  $TE=20$  ms, pH 7.2, 50 mm in a 250 mL beaker, 2.0 T), (c) linebroadened version of spectrum (b), and (d)  $^1\text{H}$  NMR spectrum of human brain *in vivo* localized in the parietal white matter of a 4-year-old patient without pathological findings (8 mL VOI,  $TE=20$  ms,  $TR=1500$  ms, 256 scans, 2.0 T).

inositol and taurine, respectively. In both cases, considerable lineshape variations are observed in going from a 7.0 T FID spectrum (Figs 2(a), 3(a)) to a 2.0 T localized STEAM spectrum at an echo time of  $TE=20$  ms (Figs 2(b), 3(b)). The 8 mL VOI was chosen inside a 250 mL beaker of an aqueous metabolite solution positioned in the center of the whole-body magnet. These conditions correspond to the situation encountered for *in vivo*  $^1\text{H}$  NMR studies of human brain.

For *myo*-inositol the main resonance at 3.56 ppm originates from a collapse of the H1, H3 and H4, H6 multiplets seen at 7.0 T.<sup>22</sup> The intensity of the distorted H5 triplet at 3.28 ppm is significantly reduced at 2.0 T, while the less strongly coupled H2 triplet at 4.06 ppm remains. In the taurine spectrum the distorted N-CH<sub>2</sub> (3.26 ppm) and S-CH<sub>2</sub> (3.43 ppm) triplets at 7.0 T merge to an apparent quartet at 2.0 T with effective chemical shifts of 3.26, 3.32, 3.38, and 3.43 ppm.

The spectra in Figs 2(c), 3(c) represent artificially linebroadened versions of the 2.0 T metabolite spectra

in Figs 2(b), 3(b) to mimic the *in vivo* linewidths and the influence of limited resolution. Obviously, the enhanced filtering by Gaussian multiplication (3.6 Hz linebroadening) results in improved signal-to-noise ratios, while the peak intensities of the sharp resonances in Figs 2(b), 3(b) drop when using the same amplitude scale. The lower parts of Figs 2, 3 offer a comparison between the linebroadened metabolite spectra and *in vivo*  $^1\text{H}$  NMR brain spectra (8 mL VOI,  $TE=20$  ms) of a 4-year-old child (Figs 2(d), 3(d)). In fact, both inositol and taurine resonances were found to be higher in spectra obtained from children than from adults. The spectrum in Fig. 2(d) was localized in the thalamus, while Fig. 3(d) refers to a location in the parietal white matter of one hemisphere.

It should be noted that the *in vivo* resonances of inositol and taurine partially overlap those from other metabolites. This particularly applies to the taurine resonances at 3.26 and 3.32 ppm which in most cases are covered by the choline-containing signals at 3.22 ppm as, for example, seen in the spectrum of the adult human brain shown in Fig. 1(d). The weak resonances of inositol at 3.65 and 3.77 ppm overlap with the 3.68 and 3.75 ppm resonances of the less strongly coupled  $\alpha$ -CH triplet of glutamate (see below). It is further noteworthy that the *in vivo* resonance linewidths are significantly broader than those obtained from metabolite solutions under identical experimental conditions. Thus, the resolution of the human brain spectra presented here is determined by biological susceptibility differences rather than limited by magnetic field inhomogeneities of the whole-body magnet.

The origin of the *in vivo* inositol signal is expected to be largely due to *myo*-inositol. Significant contributions from inositol headgroups of membrane-bound phospholipids<sup>23</sup> or inositol phosphate<sup>24</sup> can be excluded on the basis of their different  $^1\text{H}$  NMR spectra, e.g., for the chemical shift of the H2 resonance at 4.06 ppm. This finding is further supported by the fact that homonuclear off-resonance irradiation did not show a decrease of any  $^1\text{H}$  NMR visible metabolite resonances in the human brain, while the water signal was considerably reduced by a transfer of saturated magnetization from macromolecular structures to neighboring water molecules. Thus, the observed inositol resonances are not in close contact with immobilized membrane structures as would be the case for phospholipid inositols.

### Glutamate and *N*-acetyl aspartate

The methylene resonances of both glutamate and the aspartyl group of NAA represent further examples of strongly spin-coupled multiplet patterns at 2.0 T. The fully relaxed, localized STEAM spectra (8 mL VOI,  $TE=20$  ms) shown in Fig. 4 are from aqueous model solutions of glutamate (Fig. 4(a)) and a 1:1 mixture of glutamate and NAA (Fig. 4(b)). Obviously, the apparently low 'visibility' of glutamate relative to the single methyl resonance of NAA at 2.01 ppm may be entirely attributed to a distribution of its intensities into a large number of multiplet resonances. In the linebroadened version shown in Fig. 4(c), the glutamate spectrum yields four major resonance lines at 2.12, 2.18, 2.28, and 2.36 ppm in addition to three resonances from the

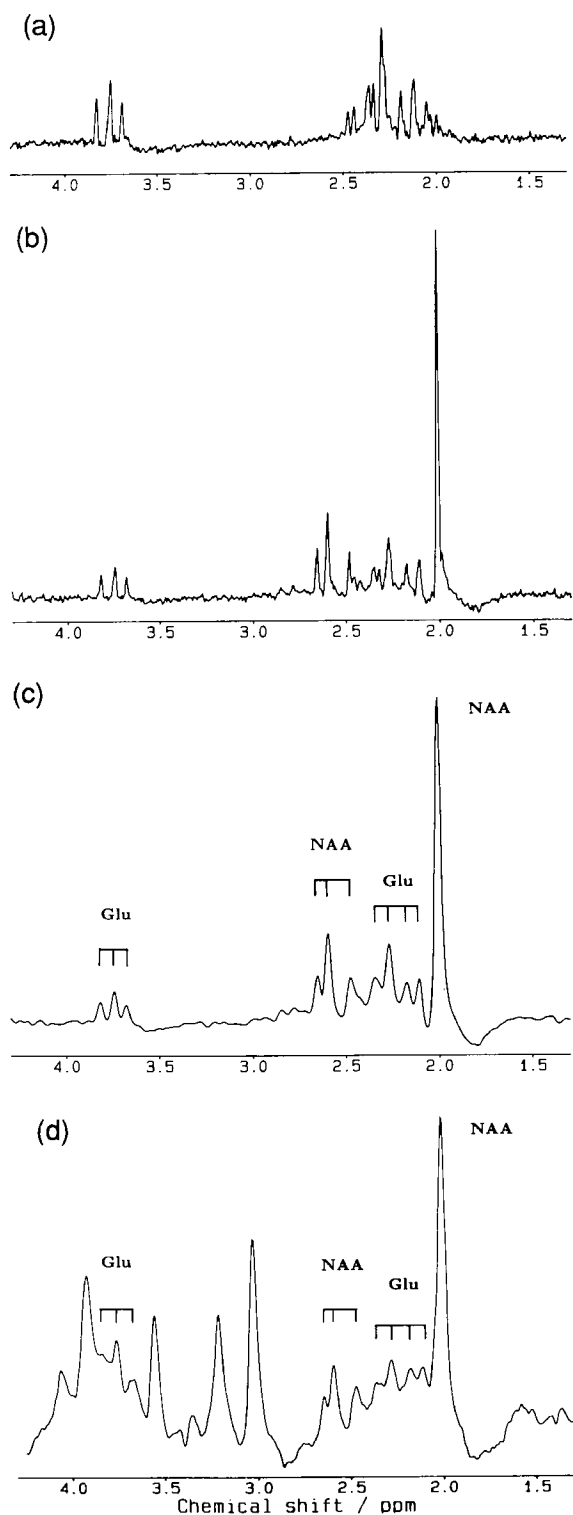


**Figure 4.** 2.0 T localized  $^1\text{H}$  NMR spectra of aqueous solutions of (a) glutamate and (b, c) mixtures of glutamate and NAA in comparison to (d) a  $^1\text{H}$  NMR spectrum of human brain *in vivo*: (a) fully relaxed, localized STEAM spectrum of glutamate (8 mL VOI,  $TE=20$  ms, pH 7.2, 50 mm in a 250 mL beaker), (b) fully relaxed, localized STEAM spectrum of a 1:1 mixture of glutamate and NAA (8 mL VOI,  $TE=20$  ms, pH 7.2, both metabolites at 50 mm in a 250 mL beaker), (c) linebroadened version of spectrum (b), and (d)  $^1\text{H}$  NMR spectrum of human gray matter *in vivo* localized in a mid-sagittal position of the parietal lobe of a 56-year-old volunteer (18 mL VOI,  $TE=20$  ms,  $TR=3000$  ms, 128 scans).

NAA aspartyl group at 2.48, 2.60 and 2.66 ppm. All these resonances as well as the less strongly coupled  $\alpha\text{-CH}$  triplet of glutamate centered at 3.75 ppm are

clearly identifiable in  $^1\text{H}$  NMR spectra of human brain. This not only applies to the *in vivo* spectrum of a 56-year-old volunteer as shown in Fig. 4(d) where the VOI was localized in the occipital gray matter in a mid-sagittal position of the parietal lobe, but also to other brain spectra from gray and white matter shown in Figs 1(d)–3(d) and 6(d), respectively.

The obvious coincidence between the NAA/glutamate model solution and the *in vivo* findings has consequences for a discussion of the relative concentrations of NAA and glutamate in human brain *in vivo*. First of all, the relative intensities of the NAA aspartyl signals are in full agreement with the intensity of the NAA singlet resonance at 2.01 ppm. The *in vivo* findings have been further confirmed by the acquisition of fully relaxed spectra ( $TR=6000$  ms) from parietal white matter in 20–30-year-old volunteers (20 cases). Thus, the 2.01 ppm signal must be entirely attributed to NAA unless another mobile metabolite exists that exhibits an identical resonance pattern but which is not detectable in tissue extracts. Secondly, despite the fact that glutamate yields significantly lower resonance signals than NAA, its concentration is only slightly lower than that of NAA. This finding is supported by a qualitative comparison of respective lineshapes and intensity ratios of the 1:1 NAA/glutamate spectrum in Fig. 4(c) with the *in vivo* spectral behavior shown in Figs 1(d)–4(d) and 6(d). Thirdly, no glutamine resonances are detectable in normal human brain *in vivo*. Based on the actually achieved signal-to-noise ratio the *in vivo* glutamine level must be at least five times lower than that of glutamate (see also below).

### Glutamine

The low level of cerebral glutamine in normal human brain means that there is considerable potential for its detection in pathological circumstances. In analogy to previous figures, this section outlines the glutamine spectral behavior at 2.0 T under the experimental conditions of a STEAM localization sequence. Figures 5(a), (b) depict fully relaxed, localized STEAM spectra of an aqueous model solution of glutamine (8 mL,  $TE=20$  ms) and its linebroadened version, respectively. The resulting pattern comprises four major resonance signals at 2.06, 2.16, 2.37, and 2.45 ppm. The latter two resonances and their corresponding amplitudes differ sufficiently from both the  $\gamma\text{-CH}_2$  resonances of glutamate and the NAA aspartyl pattern. This finding allows the identification of glutamine in the presence of NAA and glutamate, and provides the basis for a determination of their relative contributions.

This capability is demonstrated in Fig. 5(c). The spectrum represents a line-broadened version of a 1:1:1 mixture of glutamine, glutamate, and NAA (8 mL VOI,  $TE=20$  ms) and may be directly compared to the binary mixture of glutamate and NAA depicted in Fig. 4(c). While the glutamate and glutamine triplet resonances (3.75 ppm, 3.77 ppm) as well as the effective  $\beta\text{-CH}_2$  resonances overlap in a constructive way relative to the NAA intensities at 2.01 and 2.60 ppm, the presence of glutamine is clearly manifested by its overlap to the 2.48 ppm NAA aspartyl resonance and the 2.36 ppm  $\gamma\text{-CH}_2$  resonance of glutamate. This results in a characteristic change of the multiplet pattern relative

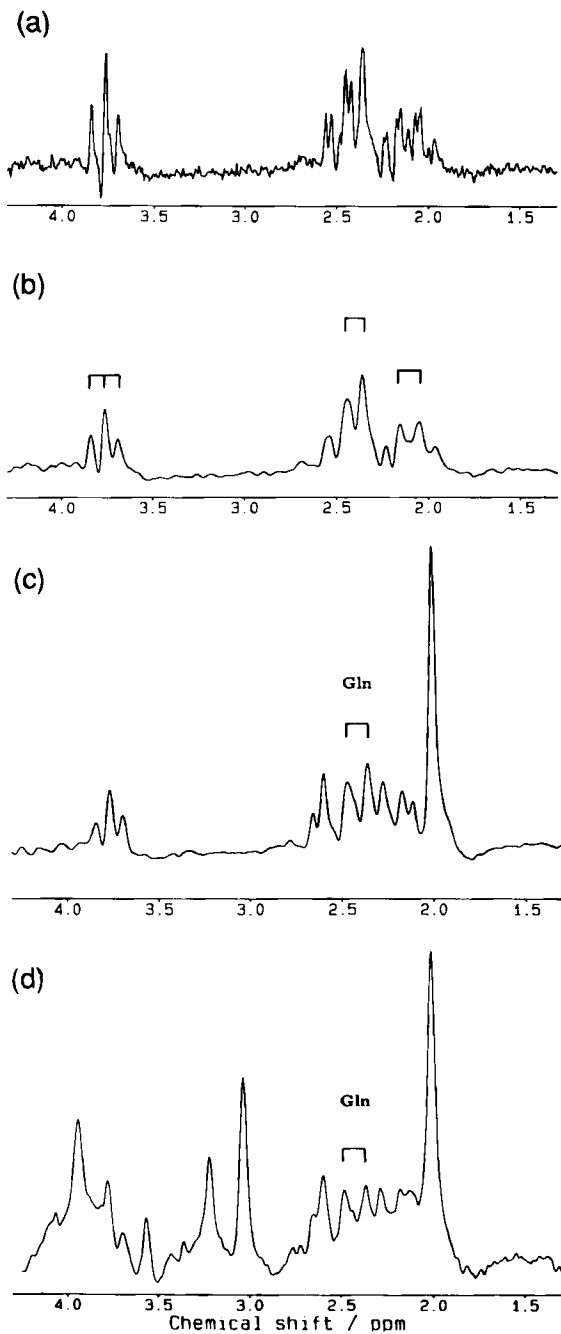


**Figure 5.** 2.0 T localized  $^1\text{H}$  NMR spectra of aqueous solutions of (a, b) glutamine and (c) a mixture of glutamine, glutamate, and NAA in comparison to (d) a  $^1\text{H}$  NMR spectrum of human brain *in vivo*: (a) fully relaxed, localized STEAM spectrum of glutamine (8 mL VOI,  $TE = 20$  ms, pH 7.2, 50 mm in a 250 mL beaker), (b) line-broadened version of spectrum (a), (c) line-broadened version of a fully relaxed, localized STEAM spectrum of a 1:1:1 mixture of glutamine, glutamate, and NAA (8 mL VOI,  $TE = 20$  ms, pH 7.2, all metabolites at 50 mm in a 250 mL beaker), and (d)  $^1\text{H}$  NMR spectrum of human gray matter *in vivo* localized in a mid-sagittal position of the parietal lobe of a 27-year-old patient presenting with liver cirrhosis (18 mL VOI,  $TE = 20$  ms,  $TR = 3000$  ms, 128 scans).

to that observed in Fig. 4(c) as well as in all other human brain spectra shown in this paper (Figs 1(d)–4(d), 6d).

The altered glutamine/glutamate spectral pattern becomes obvious in the *in vivo* spectrum of a 27-year-old patient with liver cirrhosis of infectious origin shown in Fig. 5(d). The increase of cerebral glutamine was detected by localizing (18 mL VOI,  $TE = 20$  ms) in

an occipital gray matter region similar to that used in Fig. 4(d). With references to the 1:1 ratio of glutamine to glutamate in Fig. 5(c), the relative concentration of glutamine in the patient is estimated to be about 75% of the glutamate concentration. It is believed that severe liver damage may cause an increase of ammonia in the systemic blood pool leading to an increased synthesis of glutamine in astrocytes, i.e., in gray matter regions of the brain. A full report on the alterations of cerebral metabolites in patients with severe liver diseases will be given elsewhere. A case report on the increase of cerebral glutamine in hepatic encephalopathy has been published by Kreis *et al.*<sup>25</sup>

#### Intracellular brain glucose

None of the previous  $^1\text{H}$  NMR spectra of human brain *in vivo* exhibited intracellular brain glucose levels that were sufficiently high to be detected. However, patients with diabetes suffer from elevated blood glucose concentrations that may lead to an enhanced brain glucose concentration. The  $^1\text{H}$  NMR spectrum of glucose is already strongly coupled at a field strength of 7.0 T as shown in Fig. 6(a). In close analogy to the observations for inositol and taurine in Figs 2 and 3, the fully relaxed, localized 2.0 STEAM spectrum of an aqueous solution of glucose (8 mL VOI,  $TE = 20$  ms) shown in Fig. 6(b) differs significantly from the high-field results. In particular, the signal at about 3.25 ppm almost vanishes, while the remaining complex spectral ranges simplify to an apparent singlet at 3.43 ppm and an apparent triplet at 3.80 ppm.

In order to relate the glucose resonance intensities to those of other cerebral metabolites, Fig. 6(c) shows a linebroadened version of a fully relaxed, localized 2.0 T STEAM spectrum (8 mL,  $TE = 20$  ms) of an aqueous solution of a 1:2 mixture of glucose and NAA. These results may be compared to the *in vivo* spectrum of a 69-year-old diabetic shown in Fig. 6(d). Elevated glucose levels were found when localizing (18 mL VOI,  $TE = 20$  ms) to a gray matter region in a mid-sagittal position of the occipital part of the parietal lobe. The 3.43 ppm resonance of glucose clearly overlaps with a taurine resonance at the same chemical shift, while the apparent triplet at 3.80 ppm adds to the  $\alpha$ -CH triplet of glutamate.

The patient presented with a blood glucose level of 8.3 mM. According to the model solutions and in particular with reference to the spectrum shown in Fig. 6(c), the observed glucose intensity corresponds to an intracellular concentration of about 50% of the NAA concentration, i.e., about 9 mM assuming a 10 mM concentration of total creatine (see below). A more detailed study of the regional distribution and absolute concentrations of brain glucose in patients with diabetes as well as the correlation with plasma values will be reported elsewhere. Enhanced levels of brain glucose were also found in cerebral tumors (e.g., astrocytomas) and surrounding edematous tissues<sup>2</sup> as well as in the cerebrospinal fluid *in vivo* from a VOI localized in the ventricles.

#### Summary of chemical shifts at 2.0 T

A summary of the chemical shifts of cerebral metabolites as observed in  $^1\text{H}$  NMR spectra of human brain *in vivo* is given in Table 1 for a field strength of 2.0 T. The

chemical shifts of singlet resonances and of weakly coupled multiplet resonances are field-independent and therefore agree with the data obtained at higher fields. On the other hand, the values reported for strongly

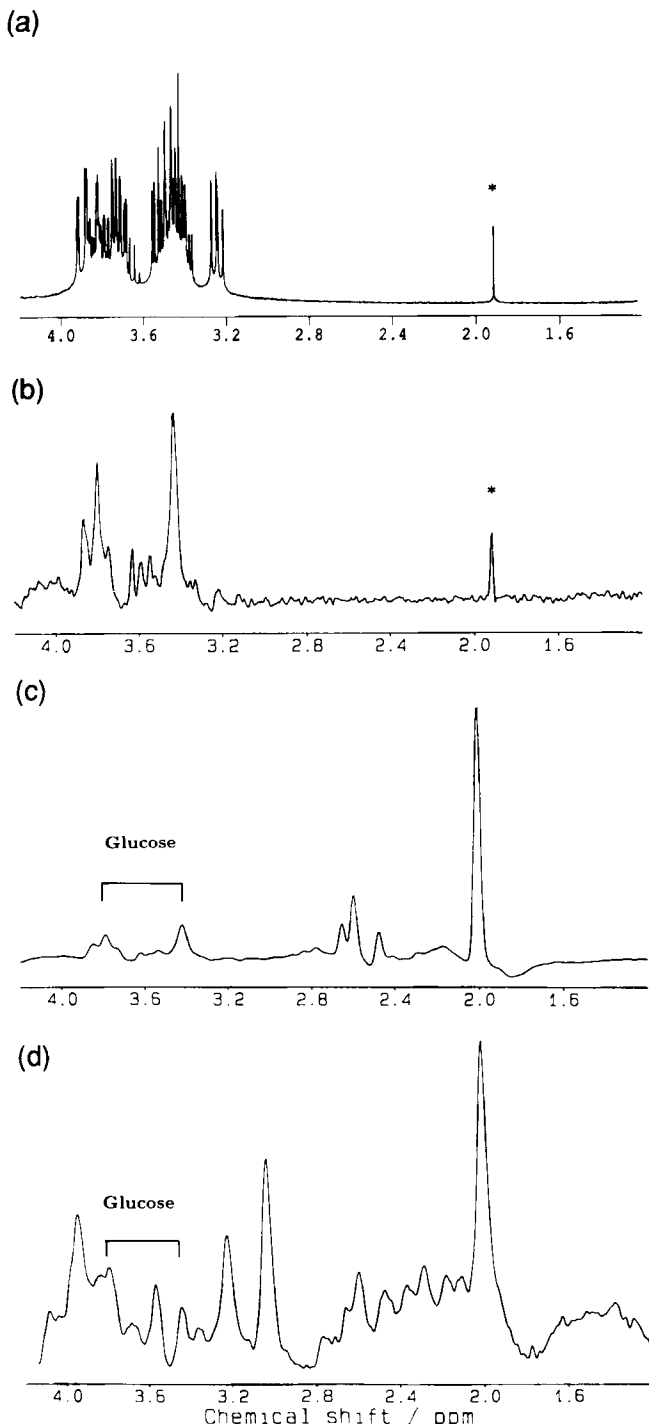


**Figure 6.**  $^1\text{H}$  NMR spectra of an aqueous solution of glucose at (a) 7.0 T and (b, c) 2.0 T in comparison to (d) a 2.0 T  $^1\text{H}$  NMR spectrum of human brain *in vivo*: (a) fully relaxed FID spectrum of glucose (pH 7.2, 50 mM, 7.0 T, \* acetate reference), (b) fully relaxed, localized STEAM spectrum of glucose (8 mL VOI,  $TE=20$  ms, pH 7.2, 15 mm in a 250 mL beaker, 2.0 T, \* acetate reference), (c) fully relaxed, localized STEAM spectrum of a 1:2 mixture of glucose and NAA (8 mL VOI,  $TE=20$  ms, pH 7.3, 15 mm glucose and 30 mm NAA in a 250 mL beaker, 2.0 T), (c) linebroadened version of spectrum (b), and (d)  $^1\text{H}$  NMR spectrum of human gray matter *in vivo* localized in a mid-sagittal position of the parietal lobe of a 69-year-old patient with diabetes mellitus presenting with a plasma glucose level of 8.3 mm (18 mL VOI,  $TE=20$  ms,  $TR=3000$  ms, 128 scans, 2.0 T).

**Table 1.** Chemical shifts  $\delta$  and multiplicities  $m$  of  $^1\text{H}$  NMR resonances of cerebral metabolites as detected in 7.0 T FID spectra of model solutions and in 2.0 T localized STEAM spectra ( $TE=20$  ms) of human brain *in vivo*

Metabolite	Molecular group	$\delta^a, m^b$	
		7.0 T	2.0 T
Lactate	$\text{CH}_3$	1.33,d	1.33
Alanine	$\text{CH}_3$	1.48,d	1.48
NAA	$\text{CH}_3$	2.01,s	2.01
Glutamate	$\text{CH}_2$	2.49/2.67,dd/dd	<u>2.48/2.60/2.66</u>
	$\beta\text{-CH}_2$	2.09,c	<u>2.00/2.05/2.12/2.18</u>
	$\gamma\text{-CH}_2$	2.36,t	<u>2.28/2.36/2.45</u>
Glutamine	$\alpha\text{-CH}$	3.75,c	<u>3.68/3.75/3.82</u>
	$\beta\text{-CH}_2$	2.13,c	<u>1.97/2.06/2.16/2.24</u>
	$\gamma\text{-CH}_2$	2.45,t	<u>2.37/2.45/2.55</u>
PCr/Cr	$\alpha\text{-CH}$	3.77,c	<u>3.70/3.77/3.85</u>
	$\text{CH}_3$	3.05,s/3.03,s	3.03
	$\text{CH}_2$	3.96,s/3.93,s	3.94
Cholines	$\text{N-(CH}_3)_3$	3.19–3.25	3.22
Taurine	$\text{N-CH}_2/\text{S-CH}_2$	3.26,t/3.43,t	<u>3.26/3.32/3.38/3.43</u>
Glucose	H2-6	3.21–3.93,c	<u>3.43/3.80</u>
<i>myo</i> -Inositol	H5	3.28,t	3.28
	H1,3/H4,6	3.52,dd/3.62,t	<u>3.56/3.65/3.77</u>
	H2	4.06,t	<u>4.06</u>

<sup>a</sup> Chemical shifts are given in ppm and referenced to 2.01 ppm for the  $\text{CH}_3$  resonance of *N*-acetyl aspartate (NAA).

<sup>b</sup> s: Singlet, d: doublet, t: triplet, dd: two doublets, c: complex.

<sup>c</sup> Major resonances of strongly spin-coupled multiplets are underlined. The spectral resolution corresponds to  $\pm 0.01$  ppm.

spin-coupled resonances refer to the *effective* chemical shifts of *apparent* resonance lines representing the distorted multiplets as they appear at 2.0 T. Since these shifts depend on the actual field strength, their identification has to be repeated for other field strengths. Although similar results may be expected, even minor field changes lead to slightly different spectral patterns as has been observed at 2.35 T in localized STEAM spectra ( $TE=20$  ms) of rat brain *in vivo*.<sup>14</sup>

It should be noted that field strengths of 4 to 7 T will be unable to solve the problem of strong coupling for inositol, taurine, glutamate, glutamine, and glucose. In fact, higher fields may introduce even more complications for an unambiguous identification of tissue metabolites due to an increased sensitivity to motion and susceptibilities. They also tend to increase the number of resonance lines and therefore complicate the resulting multiplet patterns. On the other hand, low field strengths in the 1.5 to 2.35 T range generally lead to a significant spectral simplification as demonstrated in Figs 1–6.

## CONCLUSION

The identification problems associated with spectral alterations in  $^1\text{H}$  NMR spectra at low fields versus high fields, may be overcome by qualitative assignments through lineshape comparisons of spectra obtained of metabolite solutions *in vitro* and of human brain *in vivo*, respectively. However, since even minor variations of the field strength may cause spectral changes in the presence of *strong* spin–spin coupling, the present

data are only valid for a field strength of 2.0 T. Another consequence of the results is that, with the prominent exception of lactate, *homonuclear* editing techniques with evolution periods of the order of  $1/J$  will not be applicable to cerebral metabolites. Their unavoidable  $T_2$  losses and the incomplete refocusing of multiplets due to complex  $J$  modulation are clearly demonstrated in Fig. 1.

The identification and detailed understanding of the spectral appearance of a particular metabolite is a prerequisite for a quantification of its absolute concentration *in vivo*. Current efforts focus on the establishment of the biological reproducibility, the regional distribution, the age dependence, and the physiological variability of brain spectra using a large number of volunteers. In addition, alternative strategies are tested for consistency of absolute metabolite quantifications. So far, *relative* concentrations of cerebral metabolites may be reported that are based on a comparison of metabolite spectra with fully relaxed ( $TR = 6000$  ms, 20 cases)  $^1H$  NMR spectra of white matter in the parietal lobe of young adults. Assuming total creatine

to be about 10 mM, the relative values are 18.9 mM for NAA, 3.2 mM for cholines, 11.1 mM for glutamate, 7.0 mM for inositol, and 7.4 mM for taurine. The concentrations of glutamine and glucose are too low to be detected under normal conditions. Cerebral lactate varies depending on the physiological state.

The various studies described above are necessary prerequisites for the undertaking of *meaningful* clinical trials. Anything less may compromise results and thereby jeopardize the development of *in vivo* NMR spectroscopy as a unique tool for noninvasive metabolic studies in man.

### Acknowledgements

Financial support by the Bundesminster für Forschung und Technologie (BMFT) of Germany (Grant 01 VF 8608/6) is gratefully acknowledged. We thank Dr Brian Ross for his invitation to present parts of this manuscript at the Mini-Categorical Course on Proton Spectroscopy during the 9th Annual Meeting of the Society of Magnetic Resonance in Medicine in New York, 1990. We thank Professor Dr G. Brunner for allowing us to study his patients.

### REFERENCES

- Frahm, J., Michaelis, T., Merboldt, K. D., Bruhn, H., Gyngell, M. L. and Hänicke, W., Improvements in localized proton NMR spectroscopy of human brain. Water suppression, short echo times, and 1 mL resolution. *J. Magn. Reson.* **90**, 453–464 (1990).
- Bruhn, H., Merboldt, K. D., Michaelis, T., Gyngell, M. L., Hänicke, W. and Frahm, J., Tissue heterogeneity and metabolic resolution in localized proton MRS studies of patients with cerebral tumors. *9th Annual Meeting of the Society of Magnetic Resonance in Medicine*, Abstract, p. 104, New York, NY, USA (1990).
- Bruhn, H., Frahm, J., Merboldt, K. D., Gyngell, M. L., Hänicke, W., Christen, H. J. and Hanefeld, F., Metabolic alterations in children with multiple sclerosis as detected by localized proton MRS studies. *9th Annual Meeting of the Society of Magnetic Resonance in Medicine*, Abstract, p. 1209, New York, NY, USA (1990).
- Bruhn, H., Gyngell, M. L., Merboldt, K. D., Hänicke, W. and Frahm, J., A fast scan protocol for MRI of brain lesions in less than 10 minutes. *9th Annual Meeting of the Society of Magnetic Resonance in Medicine*, Abstract, p. 186, New York, NY, USA (1990).
- Arús, C., Chang, Y. and Bárány, M., Proton nuclear magnetic resonance spectra of excised rat brain. Assignment of resonances. *Physiol. Chem. Phys. Med. NMR* **17**, 23–33 (1983).
- Behar, K. L., den Hollander, J. A., Stromski, M. E., Ogino, T., Shulman, R. G., Petroff, O. A. C. and Prichard, J. W., High-resolution  $^1H$  nuclear magnetic resonance study of cerebral hypoxia *in vivo*. *Proc. Natl Acad. Sci. USA* **80**, 4945–4948 (1983).
- Fan, T. W. M., Higachi, R. M., Lane, A. N. and Jardetzky, O., Combined use of  $^1H$  NMR and GC-MS for metabolite monitoring and *in vivo*  $^1H$  NMR assignments. *Biochim. Biophys. Acta* **882**, 154–167 (1986).
- Frahm, J., Bruhn, H., Gyngell, M. L., Merboldt, K. D., Hänicke, W. and Sauter, R., Localized proton NMR spectroscopy in different regions of the human brain *in vivo*. Relaxation times and concentrations of cerebral metabolites. *Magn. Reson. Med.* **11**, 47–63 (1989).
- Sauter, R., Loeffler, W., Bruhn, H. and Frahm, J., The human brain. Localized H-1 MR spectroscopy at 1.0 T. *Radiology* **176**, 221–224 (1990).
- Frahm, J., Bruhn, H., Gyngell, M. L., Merboldt, K. D., Hänicke, W. and Sauter, R., Localized high-resolution proton NMR spectroscopy using stimulated echoes. Initial applications to human brain *in vivo*. *Magn. Reson. Med.* **9**, 79–93 (1989).
- Frahm, J., Michaelis, T., Merboldt, K. D., Hänicke, Gyngell, M. L., Chien, D. W., and Bruhn, H., Localized NMR spectroscopy *in vivo*. Progress and problems. *NMR Biomed.* **2**, 188–195 (1989).
- Luyten, P. R., Bruntink, G., Stoff, F. M., Vermeulen, J. W. A. H., van der Heijden, J. I., den Hollander, J. A. and Heerschap, A., Broadband proton decoupling in human  $^{31}P$  NMR spectroscopy. *NMR Biomed.* **1**, 177–183 (1989).
- Merboldt, K. D., Chien, D., Hänicke, W., Gyngell, M. L., Bruhn, H. and Frahm, J., Localized  $^{31}P$  NMR spectroscopy of the adult human brain *in vivo* using stimulated-echo (STEAM) sequences. *J. Magn. Reson.* **89**, 343–361 (1990).
- Gyngell, M. L., Ellermann, J., Michaelis, T., Hänicke, W., Merboldt, K. D., Bruhn, H. and Frahm, J., Noninvasive  $^1H$  NMR spectroscopy of the rat brain *in vivo* using a short echo time STEAM localization sequence. *NMR Biomed.* **4**, in press.
- Luyten, P. R., Mariën, A. J. H., Heindel, W., van Gerwen, P. H. J., Herholz, K., den Hollander, J. A., Friedmann, G. and Heiss, W. D., Metabolic imaging of patients with intracranial tumors: H-1 MR spectroscopic imaging and PET. *Radiology* **176**, 791–799 (1990).
- Segebarth, C. M., Balériaux, D. F., Luyten, P. R. and den Hollander, J. A., Detection of metabolic heterogeneity of human intracranial tumors *in vivo* by  $^1H$  NMR spectroscopic imaging. *Magn. Reson. Med.* **13**, 62–76 (1990).
- Bruhn, H., Frahm, J., Gyngell, M. L., Merboldt, K. D., Hänicke, W., Sauter, R. and Hamburger, C., Noninvasive differentiation of tumors with use of localized H-1 MR spectroscopy *in vivo*. Initial experience in patients with cerebral tumors. *Radiology* **172**, 541–548 (1989).
- Berkelbach van der Sprenkel, J. W., Luyten, P. R., van Rijen, P. C., Tulleken, C. A. F. and den Hollander, J. A., Cerebral lactate detected by regional proton magnetic-resonance spectroscopy in a patient with cerebral infarction. *Stroke* **19**, 1556–1560 (1988).
- Bruhn, H., Frahm, J., Gyngell, M. L., Merboldt, K. D., Hänicke, W. and Sauter, R., Cerebral metabolism in man after acute stroke. New observations using localized proton NMR spectroscopy. *Magn. Reson. Med.* **9**, 126–131 (1989).
- Prichard, J., Rothman, D., Novotny, E., Petroff, O., Avison, M., Howseman, A., Hanstock, C. and Shulman, R., Photic stimulation raises lactate in human visual cortex. *8th Annual Meeting of the Society of Magnetic Resonance in Medicine*, Abstract, p. 1079, Amsterdam, Netherlands (1989).
- Sappey-Marinié, D., Calabrese, G., Hugg, J., Deicken, R., Fein, G. and Weiner, M., Increased lactate in human visual cortex during photic stimulation. *9th Annual Meeting of the*

- Society of Magnetic Resonance in Medicine*, Abstract, p. 106, New York, NY, USA (1990).
22. Cerdan, S., Parilla, R., Santoro, J. and Rico, M., <sup>1</sup>H NMR detection of cerebral *myo*-inositol. *FEBS Lett.* **187**, 167–172 (1985).
  23. Shibata, T., Uzawa, J., Sugiura, Y., Hayashi, K. and Takizawa, T., 400 MHz proton nuclear magnetic resonance studies of the polar headgroup conformation of inositol-phospholipids. *Chem. Phys. Lipids* **34**, 107–113 (1984).
  24. Cerdan, S., Hansen, C. A., Johanson, R., Inubushi, T. and Williamson, J. R., Nuclear magnetic resonance spectroscopic analysis of *myo*-inositol phosphates including inositol 1,3,4,5-tetrakisphosphate. *J. Biol. Chem.* **261**, 14676–14680 (1986).
  25. Kreis, R., Farrow, N. and Ross, B. D., Diagnosis of hepatic encephalopathy by proton magnetic resonance spectroscopy. *Lancet* **ii**, 635–636 (1990).